



# *Amsacta moorei* entomopoxvirus encodes a functional heparin-binding glycosyltransferase (AMV248)

Cihan Inan<sup>1,2</sup> · Hacer Muratoglu<sup>2</sup> · Basil M. Arif<sup>3</sup> · Zihni Demirbag<sup>1</sup>

Received: 8 February 2018 / Accepted: 9 April 2018 / Published online: 17 April 2018  
© Springer Science+Business Media, LLC, part of Springer Nature 2018

## Abstract

*Amsacta moorei* entomopoxvirus (AMEV) infects certain lepidopteran and orthopteran insects and is the most studied member of the genus *Betaentomopoxvirus*. It has been considered as a potential vector for gene therapy, a vector to express exogenous proteins and a biological control agent. One of its open reading frames, *amv248*, encodes a putative glycosyltransferase and is the only known attachment protein conserved in AMEV and chordopoxviruses. The ORF was successfully expressed and the protein was shown to bind soluble heparin, both in silico and in vitro. Our results also showed that, while viral infection was inhibited by soluble glycosaminoglycans (GAGs), GAG-deficient cells were more resistant to the virus. Finally, we revealed that *amv248* encodes an active heparin-binding glycosyltransferase which is likely to have a key role in the initiation of infection by AMEV.

**Keywords** *Amsacta moorei* entomopoxvirus · Glycosyltransferase · *amv248* · Heparin binding · Virus attachment

## Introduction

Poxviruses are large, complex, double-stranded DNA viruses that replicate in the cytoplasm of infected cells and are also known as nucleocytoplasmic large DNA viruses (NCLDV). Recently, it was suggested to include poxviruses as a member of a new virus order *Megavirales* [1]. The family *Poxviridae* comprises two subfamilies depending on their hosts; members of the *Chordopoxvirinae* and *Entomopoxvirinae* infect vertebrates and invertebrates, respectively [2]. Entomopoxviruses are further subdivided into three genera, the *Alphaentomopoxvirus*, *Betaentomopoxvirus*, and *Gammaentomopoxvirus*. *Amsacta moorei* entomopoxvirus (AMEV) is one of the few entomopoxviruses that replicates

and can be manipulated in insect cell lines such as those derived from *Lymantria dispar* (Ld652) [3] and *Estigmene acrea* (EAA-BTI) [4, 5]. The viral genome has been fully sequenced and consists of 232,392 bp with 294 open reading frames (ORFs) and contains inverted terminal repeats (ITRs) [6, 7]. Later, Guo and Yu re-predicted the number of ORFs and suggested that 256 ORFs encode functionally active proteins [8].

The most studied poxvirus, *Vaccinia virus* (VACV), has four proteins responsible for attachment to permissive cells but only one, H3, is conserved in all poxviruses [9]. H3 has been structurally and functionally characterized and is transcribed as an intermediate gene, and the protein is a member of the virus fusion entry complex that binds to heparan sulfate [10, 11]. It has been suggested that the AMV248 is an orthologue of VACV H3, and encodes a putative glycosyltransferase (GT) that binds to cellular glycosaminoglycan heparan sulfate and heparin [6, 7, 10, 12].

Members of the GT protein family (EC 2.4) transfer sugar moieties from a donor molecule to an acceptor [13]. The first gene-encoding ecdysteroid glucosyltransferase (*egt*) in baculoviruses was demonstrated in the *Autographa californica* nucleopolyhedrovirus (AcMNPV) [14]. Later, it was suggested that most baculoviruses encode an EGT [12]. The hormone ecdysone initiates and regulates the molting cycle in insects and is rendered inactive when EGT adds sugar

---

Edited by Lorena Passarelli.

✉ Zihni Demirbag  
zihni@ktu.edu.tr

<sup>1</sup> Department of Biology, Faculty of Sciences, Karadeniz Technical University, Trabzon, Turkey

<sup>2</sup> Department of Molecular Biology and Genetics, Faculty of Sciences, Karadeniz Technical University, Trabzon, Turkey

<sup>3</sup> Laboratory for Molecular Virology, Great Lakes Forestry Centre, Sault Ste. Marie, ON, Canada

molecules to the hormone, thus preventing larval molting [15]. The authors also explained that putative GTs encoded by EPVs (MSV206 [16] and AMV248 [6]) may function in a manner similar to bacterial GTs in lipopolysaccharide capsule biosynthesis and have an effect on virulence. Also, it was suggested that MSV206 may play a crucial role in cell surface carbohydrate modification during viral infection [16]. Other investigators showed that, among other viral protein, GT is required for entry of VACV and filoviruses into cells [17, 18]. According to recently sequenced entomopoxvirus genomes, it was revealed that entomopoxviruses infecting *Anomala cuprea*, *Adoxophyes honmai*, *Choristoneura biennis*, *Choristoneura rosaceana*, and *Mythimna separata* also encode proteins similar to AMV248 [7, 19].

While most DNA viruses replicate in the nucleus, poxviruses carry the proteins needed to initiate replication in the cytoplasm. Following virus attachment to cell receptors, fusion and entry occur to start the replication process. This step is regulated by mostly conserved proteins that form the Entry Fusion Complex (EFC). AMV248 is a conserved protein and its orthologue, VACV H3L, is responsible for attachment to glycosaminoglycans (GAGs) present at the host's cell surface [9]. For these reasons, we embarked on a study on functional characterization of AMV248. In an earlier study, we showed that *amv248* is transcriptionally active and is an intermediate gene expressed after DNA replication [20].

In this study, the three-dimensional structure of AMV248 ectodomain was modeled and the heparin-binding motifs were predicted in silico. AMV248 was expressed in a bacterial system and its binding capacity to heparin and the virus was investigated in vitro. The virus was pre-incubated with different concentrations of soluble GAGs resulting in loss of infectivity. Finally, we demonstrated that AMEV did not efficiently infect GAG-deficient Ld652 cells. Collectively, the data showed that AMV248 binds cellular heparin indicating that AMEV appears to target heparin of the surface of permissive cells.

## Materials and methods

### Cell line and viruses

*Lymantria dispar* (Ld652) cell line, used in this study, was obtained from Basil Arif (Great Lakes Forestry Centre, Canada) and maintained at 28 °C in a mixed medium (45% Grace's Insect Medium, 45% Excell 400, and 10% heat-inactivated Fetal Bovine Serum).

A spheroidin-deleted and GFP-tagged AMEV (Am $\Delta$ sph/gfp) was obtained from Dr. Richard W. Moyer (University of Florida, USA) and used to generate a stock virus

( $1.35 \times 10^7$  pfu/ml) used in this study [21]. GFP facilitated monitoring of infection by fluorescent microscopy.

### Predicted 3-dimensional structure of AMV248

The 3D structure of AMV248 ectodomain was predicted using MODELLER software with homology modeling method [22]. This method compares AMV248 ectodomain to other already interpreted 3D structures. X-ray diffraction data of VACV H3 (accession number 5EJ0) was downloaded from the Research Collaboratory for Structural Bioinformatics (RCSB) and Protein Data Bank (PDB) and used as a guide to predict the 3D structure of AMV248 [10].

### In silico heparin-binding assays

The ClusPro 2.0 protein–protein docking server was used to explore possible binding capacity of AMV248 to heparin in silico [23]. Docking analysis was done using heparin as ligand in advanced docking mode and performed for both AMV248 and H3.

### Excision of the transmembrane domain and generating an expression vector

In order to remove the transmembrane region from AMV248, the ectodomain was amplified using forward (5'-CGG GAT CCA TGG AAA ATT ATC ATA TTA TTA TAT TAA C-3') and reverse (5'-GGA ATT CTT ATG AGA TTA ACA TTA TTA TTA TAT AAA A-3') primers that included restriction enzyme sites (*Bam*HI in the forward and *Eco*RI in the reverse primer). PCR amplification was performed in a 50  $\mu$ l reaction volume with 10 ng of genomic DNA, 2.5 unit of Phusion DNA polymerase (Thermo Scientific), 5 $\times$  HF reaction buffer, 10 mM dNTPs, and 10 mM of forward and reverse primers. Amplification was performed as follows: 98 °C for 30 s, 35 cycles at 98 °C for 10 s, 60 °C for 30 s, and 72 °C for 30 s. Thereafter, the mixture was incubated at 72 °C for 10 min. The final PCR product was analyzed on a 1% agarose gel.

The amplified gene product was excised from the gel using DNA-gel cleaning kit (Macherey-Nagel), cloned into the pJET PCR cloning vector and used to transform *Escherichia coli* JM101. The recombinant vector containing *amv248* was selected on ampicillin plates, purified by Wizard Plus SV Minipreps DNA purification system (Promega) and sequenced by Macrogen Inc (Amsterdam, Netherlands).

### Expression and purification of AMV248 with polyhistidine-tagged particles

The *amv248* ectodomain in pJET vector was excised with *Eco*RI and *Bam*HI and ligated into the pET28a(+) vector.

The construct was used to transform *E. coli* BL21 (DE3) Competent cells to produce the plasmid pET-AMV248. Transformed *E. coli* cells were grown on LB agar plates containing kanamycin (50 µg/ml) and incubated at 37 °C for 16 h. A single colony was inoculated into LB medium and incubated with shaking to a concentration of 0.6 OD<sub>600</sub>. Expression was induced with 0.5 mM isopropyl-β-*D*-thiogalactopyranoside (IPTG). The culture was incubated for 4 h at 30 °C and the cells were pelleted at 5000 rpm for 10 min. The pellet was resuspended in 10 ml Tris–HCl buffer (20 mM, pH 7.5). Lysozyme (50 µl of 10 mg/ml) was added and incubated for 30 min at 30 °C. The mixture was sonicated and collected by centrifugation for 10 min at 14,000 rpm. Pelleted cell lysates were resuspended in 2 ml of Tris–HCl buffer and stored at – 80 °C until needed for protein purification.

AMV248 was purified by the MagneHis Protein Purification system (Promega, V8500) according to manufacturer's manual. Polyhistidine-tagged proteins bind to MagneHis Ni-Particles supplied with the purification system. Nickel-bound protein (100 µl) was added to 1 ml of expressed AMV248 and the bound proteins were washed three times with wash buffer. Proteins were eluted using MagneHis™ Elution Buffer and immediately separated on a 10% SDS-polyacrylamide gel.

### Heparin-binding capacity of virus and AMV248

HiTrap Heparin Columns (Ge Healthcare) were used to investigate the binding capacity of the virus and purified AMV248 to heparin [24]. Heparin-coated beads were extracted from the column and washed with phosphate-buffered saline (PBS) then with binding buffer (10 mM sodium phosphate, pH ~ 7). A 20 µl aliquot of stock virus ( $1.35 \times 10^7$  pfu/ml) or AMV248 was mixed with 50 µl of beads and gently agitated for 10 min at RT. Beads were pelleted at 14,000 rpm for 30 s, and the upper phase including unbound particles was discarded.

The beads were washed three times with binding buffer then suspended in elution buffer (10 mM sodium phosphate, 2 M NaCl, pH ~ 7) for 10 min to elute bound virus or AMV248. Purified virus and proteins were immediately separated on SDS-PAGE and analyzed on Western blots.

### SDS-PAGE and Western blot analysis

Purified AMV248 was mixed with an equal volume of 2× Laemmli Sample buffer (Bio-Rad #161-0737) including 2-mercaptoethanol. A 40 µl sample of purified virus was mixed with 10 µl Triton X-100 in PBS (0.1%) then an equal volume of Laemmli sample buffer with 2-mercaptoethanol (5%) was added. The samples were then incubated at 94 °C for 2 min. All samples were loaded and analyzed on 10%

TGX Stain-Free FastCast Acrylamide gels (Bio-Rad #161-0183). Proteins were then transferred to Mini-Size polyvinylidene fluoride (PVDF) membranes by Semi-Dry blotting (Bio-Rad). Membranes were blocked for 1 h in TTBS (50 mM Tris–HCl [pH 7.5], 150 mM NaCl, 0.05% Tween 20) with the addition of 5% (w/v) skim milk powder. Membranes were incubated overnight with mouse monoclonal anti-polyhistidine antibody (Sigma, H1029) for the protein samples or with monoclonal anti-GFP antibody (1:1000 dilution in TTBS with 0.5% milk powder. Cell Signaling, 2555) to detect the virus. Membranes were washed three times with wash buffer and incubated with anti-mouse IgG alkaline phosphatase (AP) antibody (Sigma, A3562) for the protein samples or anti-rabbit IgG AP antibody (Sigma, A3687) for the virus samples at a dilution 1:1000 in wash buffer. They were once again washed three times with wash buffer, twice with AP buffer, and analyzed by adding AP buffer containing nitro blue tetrazolium and 5-bromo-4-chloro-3-indolyl phosphate (NBT-BCIP) stock solution.

### Inhibition of infection with soluble glycosaminoglycans

Ld652 cells ( $2 \times 10^4$ ) were seeded into each well of 96-well plates and grown overnight. Aliquots of AmΔsph/gfp virus containing 300 pfu (minimum titer to track GFP production on 96-well plate—data not shown) were mixed with different concentrations (5–50 µg/ml) of soluble GAGs (heparin, heparan sulfate, chondroitin sulfate A, and dermatan sulfate) and incubated for 1 h. A 100 µl sample from the different mixtures was added to each well of cells. After 2 h, the virus inoculum was removed and replaced with 200 µl of fresh medium and incubated for 48 h. GFP expression was detected by fluorescent microscopy (Zeiss, Axiovert 200 M) and progeny virus titers were determined by the end point dilution method (EPDA) [25].

### Heparinase treatment of Ld652 cells

Ld652 cells ( $2 \times 10^4$ ) were seeded into each well of a 96-well plate and grown overnight. The cells were incubated for 1 h with 50 µl of various concentrations (0.1–0.5 unit/well) of Heparinase I in 20 mM Tris–HCl, pH 7.5, 4 mM CaCl<sub>2</sub>, 50 mM NaCl, and 0.01% BSA or Heparinase III in 20 mM Tris–HCl, pH 7.5, 4 mM CaCl<sub>2</sub>, and 0.01% BSA (Sigma) to digest cellular heparins and heparan sulfates, respectively. Also, non-treated cells were used as negative controls. All groups were washed twice with PBS and infected with 300 pfu of AmΔsph/gfp virus. After 2 h, the inoculum was replaced with fresh medium and incubated for 48 h. GFP expression was detected by fluorescent microscopy (Zeiss, AxioVert 200 M). Progeny virus titer was determined by the end point dilution (EPDA) method (Fig. 6) [25].

## Results

### Bioinformatics analysis

The 870 bp of ORF *amv248* potentially encodes a protein of 279 amino acids. Analysis was performed to identify conserved regions, transmembrane domain, and a signal peptide. The data revealed that while the protein has a glycosyltransferase domain, no signal peptide was detected. All protein-binding studies (in vitro and in silico) were performed with AMV248 without the transmembrane region.

### AMV248 was modeled to bind soluble heparin

Viral attachment proteins usually target cellular glycosaminoglycans (GAGs) as the initial step to gain access into the host cells [26]. Although VACV has 3 proteins targeting different GAGs, AMEV has only one (AMV248) that putatively binds heparin. To ascertain binding, we first generated a 3D structure of AMV248 using homology modeling (Fig. 1). This method requires a known X-ray structure of a template molecule to propose a structure of a test protein. The sequence and 3D structure of H3 (pdb 5EJ0) of VACV were the template to predict the structure of AMV248. The 3D model of AMV248 was designed and aligned with H3 using PyMol software (Fig. 1) and revealed that both 3D designs have similar Ramachandran plots (Fig. 2, [27]). The ClusPro 2.0 server (<http://cluspro.org>) was used to predict the docking of the 3D model of AMV248 with heparin.

Also, H3 protein, previously reported to bind heparin was docked to validate the data. According to the generated energy scores the results showed that both AMV248 and H3 bind heparin in silico with energy scores of  $-982.4$  and  $-677.9$  kcal, respectively. All amino acids and bond types are listed in Table 1.

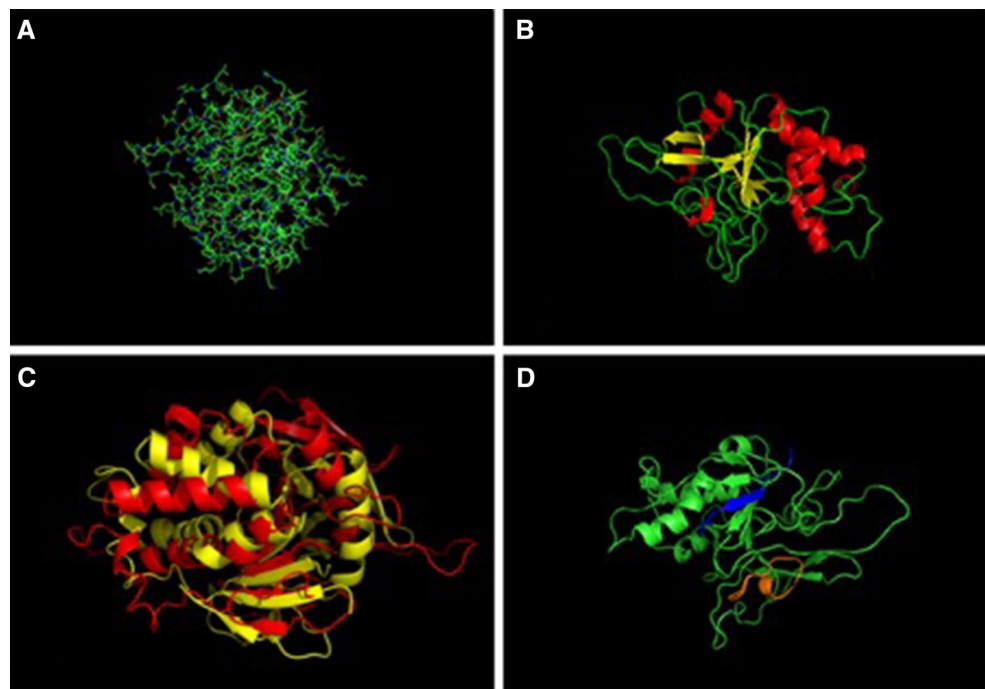
### ORF *amv248* encodes a 30 kDa glycosyltransferase

The DNA sequence encoding the ectodomain (without the transmembrane domain) was amplified, screened, and expressed in a bacterial expression vector. The vector was designed to add polyhistidine tags to the *N*-terminus to AMV248 in order to facilitate protein purification and eventual detection with specific antibodies. The expressed protein was purified with Promega MagneHis Purification system and separated on a polyacrylamide gel. Anti-poly histidine antibody detected an expected expressed protein of approximately 30 kDa (Fig. 3).

### Am $\Delta$ sph/gfp virus and AMV248 protein bind to heparin in vitro

In silico experiments and sequence similarity analysis suggested that both the virus and AMV248 bind heparin molecules. To test this hypothesis, AMV248 or recombinant virus expressing gfp was purified using heparin-bound Sepharose beads. Eluted virus or protein was separated on polyacrylamide gels and detected by western blots using anti-gfp antibody or anti-poly-histidine antibody, respectively. The results

**Fig. 1** AMV248 ectodomain 3D image generated with MODELLER software and screened with PyMol software. **a** 3D structure of AMV248 as lines, **b** 3D structure of AMV248 as cartoon (red: helix, yellow: sheet, green: loop structures). **c** Alignment of predicted AMV248 (red) and VACV-H3 (yellow) 3D structures. **d** AMV248 3D from a different angle (N-terminal end colored as blue and carboxyl end colored as orange) (Color figure online)





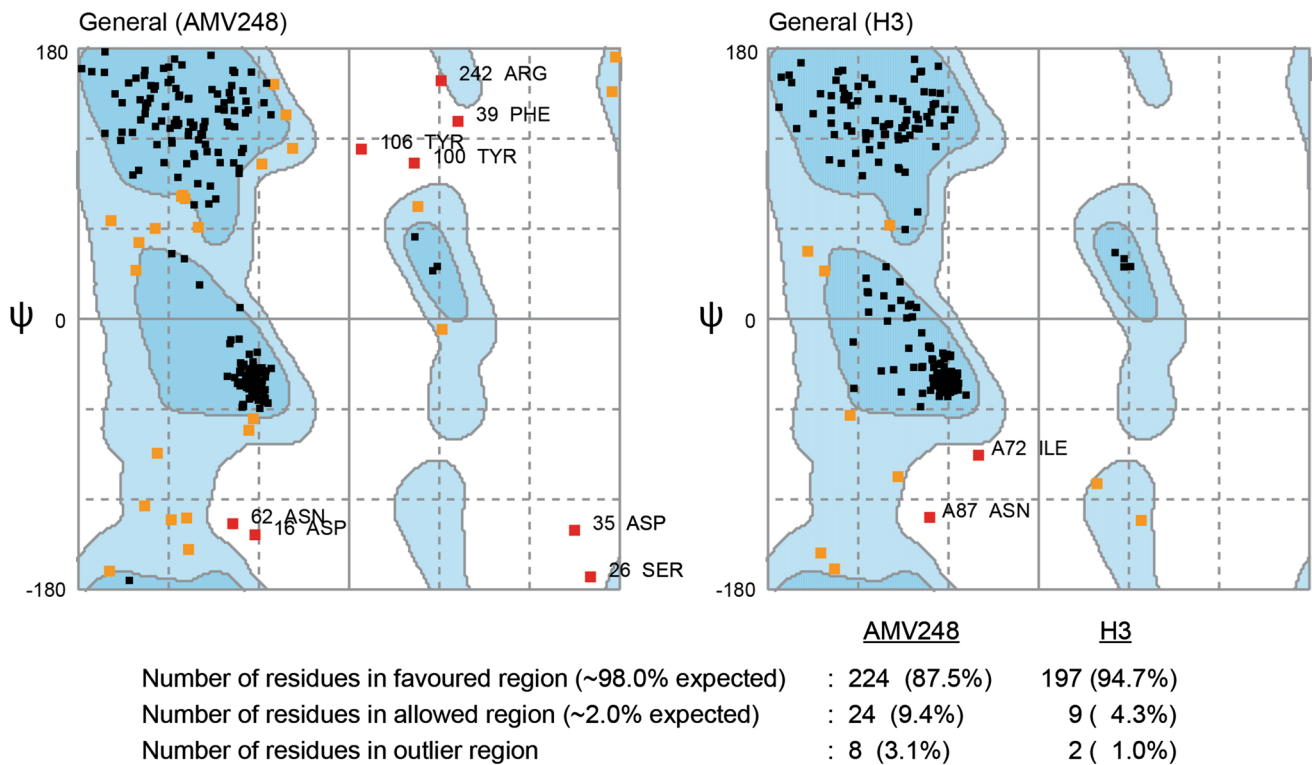


**Fig. 2** AMV248 and *Vaccinia virus* H3 proteins have similar Ramachandran plots. The AMV248 predicted 3D structure and H3 3D structure (5EJ0) were used to generate Ramachandran plots.

Results showed that while AMV248 structure has more unfavorable amino acids, none of them appear to contribute to the heparin-binding region

showed that both Am $\Delta$ sph/gfp virus and AMV248 protein did indeed bind heparin in vitro (Fig. 4).

### Soluble GAGs inhibit viral infection

As a follow up to the previous results, we needed to demonstrate that glycosaminoglycans actually bind to and inhibit virus infection. Various concentrations of different GAGs were mixed with 300 pfu of virus and added to Ld652 cells as described in “Materials and Methods.” Non-treated cells were also infected with the same amount of virus as control. Progeny virus was harvested and titers were calculated using the EPDA (not shown). The data summarized in Fig. 5 show the titers of GAG-treated samples compared to the control group. They indicate that virus infection was inhibited at each concentration of all GAGs tested. Maximum inhibition occurred at the highest concentration (50  $\mu$ g/ml) of GAGs. Inhibition of 98% occurred with heparin, chondroitin sulfate A, and dermatan sulfate. Heparan sulfate inhibited virus infection by 69%.

### Heparin-deficient Ld652 cells are more resistant to viral infection

Ld652 cells were incubated with different concentrations (0.0–0.5 unit/well) of heparinase I to cleave both heparin

and heparan sulfates or heparinase III to cleave heparan sulfates. The cells were then infected with 300 pfu of virus and progeny virus titers were assayed and compared (percent) to the negative controls (no enzyme). The data show that cells treated with the lower concentrations of heparinase I produced progeny virus comparable to the control group. There was a marked reduction in virus titer in cells treated with 0.5 units of heparinase I. Heparinase III did not appear to have an effect on progeny virus production (Fig. 6).

### Discussion

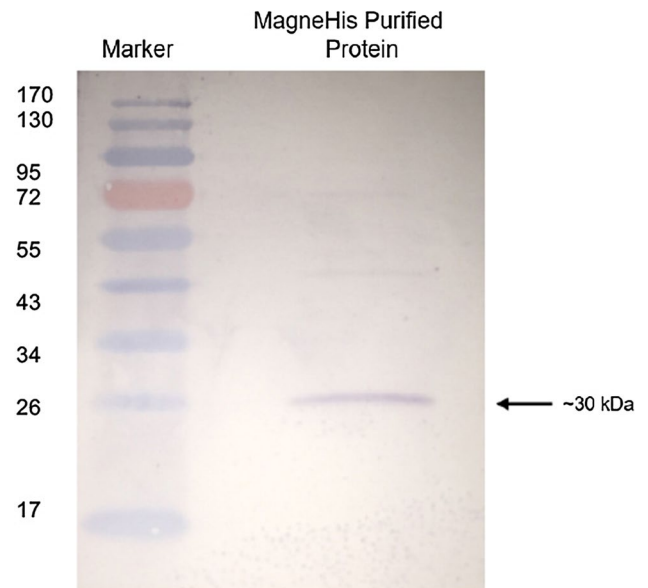
Previous studies demonstrated that many viruses initiate infection by binding to cellular GAGs [24, 28, 29]. We adopted a multi-pronged approach to study attachment to Ld652 cells in vitro and in silico including GAG-binding experiments, incubation of the virus with soluble GAGs prior to infection, and determining viral symptoms and titers in GAG-deficient cells. We focused on the *amv248* gene, potentially encoding a glycosyltransferase and may bind cellular GAG heparin [6]. Sequence analysis of *amv248* exposed two conserved regions; one belonging to the glycosyltransferase family 25 and the other is known as the poxvirus P35 protein family in which VACV H3 is a member [30].

**Table 1** Heparin-binding amino acids of AMV248 depending on docking results

Amino acid	Distance (Å)	Bond types
LYS53	1.68526	Salt bridge; attractive charge
LYS57	1.89212	Salt bridge; attractive charge
LYS57	2.15643	Salt bridge; attractive charge
LYS61	1.75059	Salt bridge; attractive charge
LYS61	1.97205	Salt bridge; attractive charge
LYS57	4.74922	Attractive charge
ASN50	2.59267	Conventional hydrogen bond
LYS57	2.07661	Conventional hydrogen bond
LYS58	2.80524	Conventional hydrogen bond
GLY59	1.92983	Conventional hydrogen bond
LYS61	1.82409	Conventional hydrogen bond
LYS61	2.09912	Conventional hydrogen bond
THR68	2.03197	Conventional hydrogen bond
SER193	2.0557	Conventional hydrogen bond
LEU194	1.9854	Conventional hydrogen bond
ASN195	2.2854	Conventional hydrogen bond
ASN211	2.08517	Conventional hydrogen bond
HIS219	2.26239	Conventional hydrogen bond
ASN220	2.8162	Conventional hydrogen bond
ASN220	2.19747	Conventional hydrogen bond
ASN220	3.08709	Conventional hydrogen bond
ASN221	2.16983	Conventional hydrogen bond
ASN221	2.27202	Conventional hydrogen bond
ASN221	2.86438	Conventional hydrogen bond
ASN221	2.21071	Conventional hydrogen bond
SER73	2.92914	Carbon hydrogen bond
SER193	3.34181	Carbon hydrogen bond
CYS56	3.77905	Carbon hydrogen bond
TYR66	4.75183	Pi-anion

While heparin-binding proteins have XBBXB or XBBBXXXBX motifs in their amino acid sequence (B being a basic amino acid and × is a neutral or hydrophobic amino acid) [31], AMV248 does not have such motifs. Also, it has been previously shown that many glycosyltransferases including H3 have D/ExD motifs [10]. AMV248 has an ExD motif, suggesting that it is an orthologue of VACV H3. Therefore, it is likely to encode a putative heparin-binding protein. The 3D structure of H3 (5EJ0) was shown to bind heparan sulfate and UDP-glucose [10]. We, therefore, determined the AMV248 3D structure using H3 as a template and focused on *in silico* analysis to elucidate binding to heparin. Docking experiments showed that both H3 and AMV248 bind cellular GAG heparin.

To determine the function of AMV248, the region encoding the ectodomain, without the transmembrane sequence, was amplified, expressed, and purified as a 30 kDa protein on PAGE then authenticated by western blots. The binding

**Fig. 3** Expressed AMV248 protein detected by western blot analysis targeting the polyhistidine tag generated with pET28(a+) bacterial expression vector system

to heparin was investigated by incubating the virus and the expressed ectodomain protein with heparin beads. Western blots determined that both had bound specifically to heparin (Fig. 4). Thus, *in silico* and actual experimental *in vitro* data indicated that the virus and AMV bind to heparin. Similar data have been reported for filoviruses [24].

We also investigated interaction between AMV248 and GAGs. The data showed that all the tested soluble GAGs interacted with AMEV even at the lowest concentration (5 µg/ml) resulting in the inhibition of virus infection. It was previously shown that cellular GAGs are targets for viral attachment [28] and that soluble GAGs have been used quite commonly to investigate viral attachment. Filoviruses clearly bind GAGs depending on virus type or host cells, and all concentrations of soluble heparin seem to inhibit viral infection [24]. Herpesviruses also target cellular heparin [29]. Studies with poxviruses demonstrated that H3 and A27 of VACV, cowpox, rabbitpox, Shope fibroma virus, and myxoma virus bind to heparan sulfate [32]. Apparently, a concentration of 50 µg/ml of soluble heparin and heparan sulfate inhibited viral infection by 90 and 60%, respectively [33].

We also found that the titer of progeny virus decreased markedly when heparin molecules were enzymatically removed from Ld652 cells. Filovirus replication was inhibited to varying levels when cells were treated with different concentrations of heparinase I and III [24]. Collectively, the data support the fact that infection of cells by AMEV is initiated by attachment of the virus to cellular heparin as has been shown for chordopoxviruses [17, 34–38].

**Fig. 4** *Amsacta moorei* entomopoxvirus and recombinant AMV248 proteins bind to heparin molecule in vitro. **a** Western blot analysis of heparin-bounded Am $\Delta$ sph/gfp virus using anti-GFP antibody. **b** Western blot analysis of HiTrap heparin-purified recombinant AMV248 using anti-polyhistidine antibody

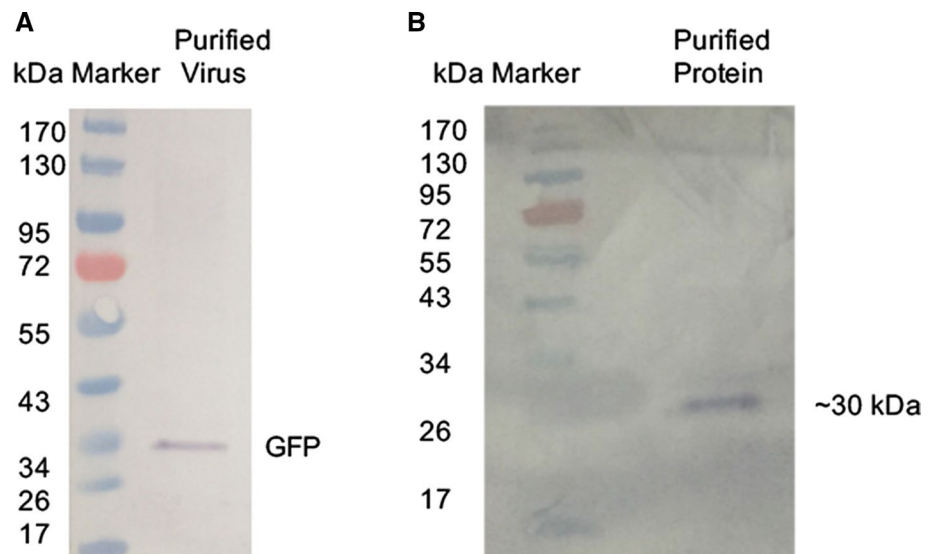


**Fig. 5** Soluble GAGs inhibited Am $\Delta$ sph/gfp virus infection in vitro. Ld652 cells were infected with 300 pfu virus in the absence of soluble GAGs. Infection ratios were calculated and compared to the control group

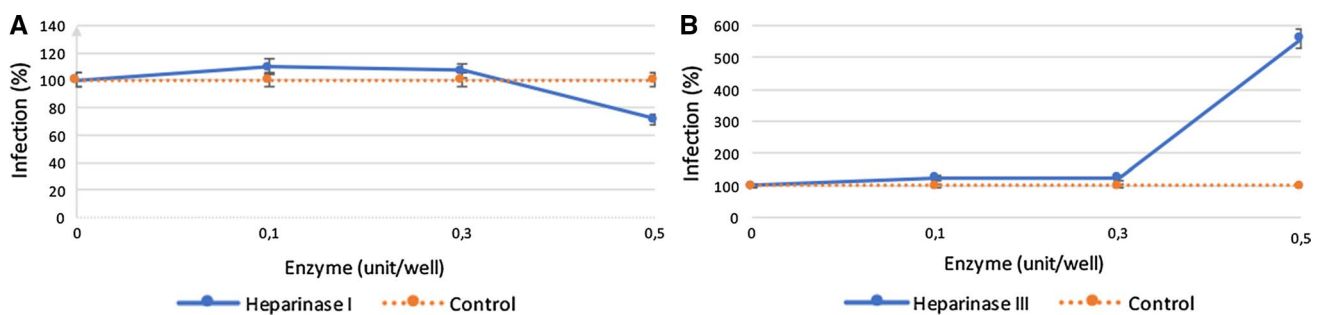
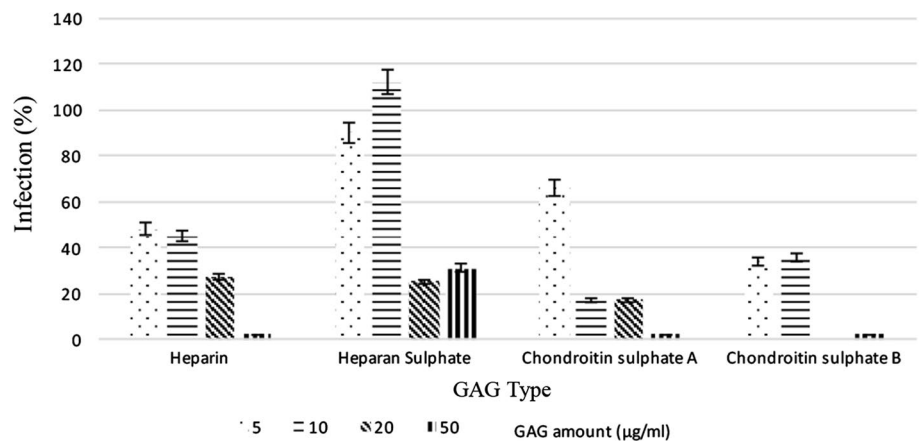


**Fig. 6** Infection of GAG-deficient Ld652 cells. Cells were treated with heparinase I (a) or heparinase III (b) then infected with 300 pfu of Am $\Delta$ sph/gfp virus. Infection percentages were calculated from EPDA

In order to facilitate entry into permissive cells, choropoxviruses have three proteins needed for attachment to cellular GAGs (H3, D8, and A27) and one to Laminin (A26) [10, 17, 32, 34, 35]. AMV248 is the only conserved attachment protein and is an orthologue of H3

with seemingly similar properties. While H3 has a role in virus assembly, this has not yet been demonstrated with AMV248. This is the first report on the characterization of an entomopoxvirus attachment protein.

Finally, we have demonstrated that *amv248* ORF of AMEV encodes a heparin-binding glycosyltransferase and suggests that heparin is the target for AMEV for the attachment to the permissive cells.

**Acknowledgements** This work was supported financially by The Scientific and Technological Research Council of Turkey, TUBITAK, [Project No. 113Z219].

**Author contributions** ZD designed the study. CI and HM performed laboratory work. BMA analyzed the data. All authors contributed to the writing of the manuscript.

## Compliance with ethical standards

**Conflict of interest** The authors declare that they have no conflict of interest.

**Ethical approval** This article does not include any studies with human participants or animals performed by any of the authors.

**Informed consent** Informed consent was obtained from all individual participants included in this article.

## References

1. P. Colson, X. De Lamballerie, N. Yutin, S. Asgari, Y. Bigot, D.K. Bideshi, X.-W. Cheng, B.A. Federici, J.L. Van Etten, E.V. Koonin, B. La Scola, D. Raoult, Arch. Virol. **158**, 2517 (2013)
2. F.I. Schmidt, C.K.E. Bleck, J. Mercer, Curr. Opin. Virol. **2**, 20 (2012)
3. J. Winter, R.L. Hall, R.W. Moyer, Virology **211**, 462 (1995)
4. R.R. Granados, M. Naughton, Intervirology **5**, 62 (1975)
5. S.A. Marlow, L.J. Billam, C.P. Palmer, L.A. King, J. Gen. Virol. **74**, 1457 (1993)
6. A.L. Bawden, K.J. Glassberg, J. Diggans, R. Shaw, W. Farmerie, R.W. Moyer, Virology **274**, 120 (2000)
7. J. Thézé, J. Takatsuka, Z. Li, J. Gallais, D. Doucet, B. Arif, M. Nakai, E.A. Herniou, J. Virol. **87**, 7992 (2013)
8. F.-B. Guo, X.-J. Yu, J. Virol. Methods **146**, 389 (2007)
9. B. Moss, Viruses **4**, 688 (2012)
10. K. Singh, A.G. Gittis, R.K. Gitti, S.A. Ostazeski, H.-P. Su, D.N. Garboczi, J. Virol. **90**, JVI.02933 (2016)
11. F.G. da Fonseca, E.J. Wolffe, A. Weisberg, B. Moss, J. Virol. **74**, 7508 (2000)
12. N. Markine-Goriaynoff, L. Gillet, J.L. Van Etten, H. Korres, N. Verma, A. Vanderplassen, J. Gen. Virol. **85**, 2741 (2004)
13. P.M. Coutinho, E. Deleury, G.J. Davies, B. Henrissat, J. Mol. Biol. **328**, 307 (2003)
14. D.R. O'Reilly, L.K. Miller, J. Virol. **64**, 1321 (1990)
15. D.R. O'Reilly, L.K. Miller, Science **245**, 1110 (1989)
16. C.L. Afonso, E.R. Tulman, Z. Lu, E. Oma, G.F. Kutish, D.L. Rock, J. Virol. **73**, 533 (1999)
17. C.-L. Lin, C.-S. Chung, H.G. Heine, W. Chang, J. Virol. **74**, 3353 (2000)
18. A. O'Hearn, M. Wang, H. Cheng, C.M. Lear-Rooney, K. Koning, E. Rumschlag-Booms, E. Varhegyi, G. Olinger, L. Rong, J. Virol. **89**, 5441 (2015)
19. W. Mitsuhashi, K. Miyamoto, S. Wada, Virology **452–453**, 95 (2014)
20. C. Inan, H. Muratoglu, B.M. Arif, Z. Demirbag, Virus Res. **243**, 25 (2018)
21. C.P. Palmer, D.P. Miller, S.A. Marlow, L.E. Wilson, A.M. Lawrie, L.A. King, J. Gen. Virol. **76**(Pt 1), 15 (1995)
22. B. Webb, A. Sali, Curr. Protoc. Protein Sci. **86**, 2 (2014)
23. D. Kozakov, D.R. Hall, B. Xia, K.A. Porter, D. Padhorny, C. Yueh, D. Beglov, S. Vajda, Nat. Protoc. **12**, 255 (2017)
24. B. Salvador, N.R. Sexton, R. Carrion, J. Nunneley, J.L. Patterson, I. Steffen, K. Lu, M.O. Muench, D. Lembo, G. Simmons, J. Virol. **87**, 3295 (2013)
25. A.J. Darling, J.A. Boose, J. Spaltro, Biologicals **26**, 105 (1998)
26. R.S. Aquino, P.W. Park, Front. Biosci. **21**, 1260 (2016)
27. S.C. Lovell, I.W. Davis, W.B. Arendall, P.I.W. de Bakker, J.M. Word, M.G. Prisant, J.S. Richardson, D.C. Richardson, Proteins Struct. Funct. Bioinform. **50**, 437 (2003)
28. E. Kamhi, E.J. Joo, J.S. Dordick, R.J. Linhardt, Biol. Rev. **88**, 928 (2013)
29. M.T. Shieh, P.G. Spear, J. Virol. **68**, 1224 (1994)
30. D.H. Davies, M.M. McCausland, C. Valdez, D. Huynh, J.E. Hernandez, Y. Mu, S. Hirst, L. Villarreal, P.L. Felgner, S. Crotty, J. Virol. **79**, 11724 (2005)
31. A. Kern, K. Schmidt, C. Leder, O.J. Müller, C.E. Wobus, C.W. Von Der Lieth, J.A. King, O.J. Mu, K. Bettinger, J. Virol. **77**, 11072 (2003)
32. C.S. Chung, J.C. Hsiao, Y.S. Chang, W. Chang, J. Virol. **72**, 1577 (1998)
33. Z. Bengali, A.C. Townsley, B. Moss, Virology **389**, 132 (2009)
34. J.C. Hsiao, C.S. Chung, W. Chang, J. Virol. **73**, 8750 (1999)
35. W.-L. Chiu, C.-L. Lin, M.-H. Yang, D.-L.M. Tzou, W. Chang, J. Virol. **81**, 2149 (2007)
36. T.G. Senkevich, S. Ojeda, A. Townsley, G.E. Nelson, B. Moss, Proc. Natl. Acad. Sci. USA **102**, 18572 (2005)
37. C.H. Foo, H. Lou, J.C. Whitbeck, M. Ponce-de-León, D. Atanasiu, R.J. Eisenberg, G.H. Cohen, Virology **385**, 368 (2009)
38. A.C. Townsley, T.G. Senkevich, B. Moss, J. Virol. **79**, 9458 (2005)